Hypoxia-induced Effects on ECG Depolarization by Time Warping Analysis during Recurrent Obstructive Apnea

Daniel Romero and Raimon Jané, *Senior Member, IEEE*

***Abstract*— In this work, we evaluated a non-linear approach to estimate morphological variations in ECG depolarization, in the context of intermittent hypoxia (IH). Obstructive apnea sequences were provoked for 15 minutes in anesthetized Sprague-Dawley rats, alternating with equal periods of normal breathing, in a recurrent obstructive sleep apnea (OSA) model. Each apnea episode lasted 15 s, while the frequency used for each sequence was randomly selected. Average heartbeats obtained before the start and at the end of each episode, were delineated to extract only the QRS wave. Then, the segmented QRS waves were non-linearly aligned using the dynamic time warping (DWT) algorithm. Morphological QRS changes in both the amplitude and temporal domains were estimated from this alignment procedure. The hypoxic and basal segments were analyzed using ECG (lead I) recordings acquired during the experiment. To assess the effects of IH over time, the changes relative to the basal QRS wave were determined, in the intervals prior to each successive events until the end of the experiment. The results showed a progressive increase in the amplitude and time-domain morphological markers of the QRS wave along the experiment, which were strongly correlated with the changes in traditional QRS markers ($r \approx 0.9$). Significant changes were found between pre-apnea and hypoxic measures only for the time-domain analysis ($p<0.001$), probably due to the short duration of the simulated apnea episodes.**

Clinical relevance **Increased variability in ECG depolarization morphology during recurrent hypoxic episodes would be closely related to the expression of cardiovascular dysfunction in OSA patients.**

I. INTRODUCTION

Repeated episodes of apnea during sleep in patients with obstructive sleep apnea (OSA), can result in a sustained exposure to intermittent hypoxia (IH). This chronic condition has been linked to some cardiovascular consequences of OSA, including systemic hypertension, myocardial infarction, and stroke among others [1], [2], [3].

The mechanisms linking IH to cardiovascular diseases in OSA patients remain unclear. Nevertheless, some specific conditions have been associated with this matter, such as an elevated sympathetic tone of the autonomic nervous system (ANS) [4], oxidative stress and endothelial dysfunction [2], inflammation and atherosclerosis [3].

To figure out the association between OSA and cardiovascular diseases, many studies have developed experimental models of acute/chronic IH. Particularly, rat models represent one of the most common used for understanding the physiological mechanisms involved in sleep apnea. Cardiovascular functions and the control handled by the autonomic nervous system (ANS) have been widely studied in this setting, through the heart rate variability (HRV) analysis [5], [6] or evaluating ECG markers for characterizing both repolarization and depolarization intervals in both amplitude and temporal domains. Apart from conventional markers, there have been proposed other ECG markers able to robustly quantify morphological changes of the ECG waveforms (QRS complex and T wave), such as the QRS slopes and angles [7] and non-linear measures derived from dynamic time warping (DTW) analysis [8].

DTW is an algorithm allowing to measure the similarity between temporal sequences that may differ in speed. It has been successfully applied in automatic speech recognition to deal with different speaking speeds, speaker recognition, and online signature recognition. Furthermore, it is seen to be useful in partial shape matching applications, which finds applications in genetic sequence and audio synchronization. These particular characteristics of DTW are exploited in this work to characterize the hypoxia-induced effects on the ECG waveforms caused by OSA. To do this, a rat model was developed by simulating recurrent apneas sequences through periodic airway obstructions [9], [10]. The model included [11] a control system to regulate the frequency and duration of the simulated apneas, while several physiological signals are being recorded to monitor cardiac and respiratory activity using different sensors.

This study aimed to assess the hypoxia-induced effects on the ECG due to recurrent OSA, using an experimental rat model. These effects were investigated after completion of several sequences of recurrent apnea concerning basal values, but also before and during hypoxic episodes to assess possible transient changes. To do this, morphology-based depolarization ECG markers quantifying both amplitude and temporal variations were investigated.

II. MATERIALS AND METHODS

A. Experimental data

The study dataset comprises six male Sprague-Dawley rats (mean weight: 437±27 g) anesthetized with urethane

*This project has received funding from the European Union's Horizon 2020 research and innovation programme under the Marie Sklodowska-Curie grant agreement No. 846636. This work was also supported by the CERCA Program/Generalitat de Catalunya, in part by the Secretaria d'Universitats i Recerca de la Generalitat de Catalunya under grant GRC 2017 SGR 01770 and in part by the spanish grant RTI2018-098472-B-I00 (MCIU/AEI/FEDER, UE).

D. Romero is with the BIOSPIN group at the Institute for Bioengineering of Catalonia (IBEC), the Barcelona Institute of Science and Technology (BIST), Barcelona, Spain (email: dromero@ibecbarcelona.eu).

R. Jané is with the Institute for Bioengineering of Catalonia (IBEC), the Barcelona Institute of Science and Technology (BIST), Centro de Investigación Biomédica en Red de Bioingeniería, Biomateriales y Nanomedicina (CIBER-BBN) and ESAII Department, Universitat Politècnica de Catalunya - BarcelonaTech (UPC), Barcelona, Spain (email: rjane@ibecbarcelona.eu).

(1g/1kg). The system to which the animals were connected incorporates a nasal mask with one tube open to the atmosphere and another connected to a positive pressure pump, thus preventing the animal from rebreathing. Obstructive apneas were simulated by closing the airways in the tubes using electrovalves, which were controlled using the Biopac® Systems. The nasal mask, electrodes, and SpO_2 sensor were placed on the anesthetized animals after shaving the specific positions (Fig 1). The animal model and experiments described here were approved by the Institutional Animal Care and Ethics Committee of the Hospital Clínic, Barcelona.

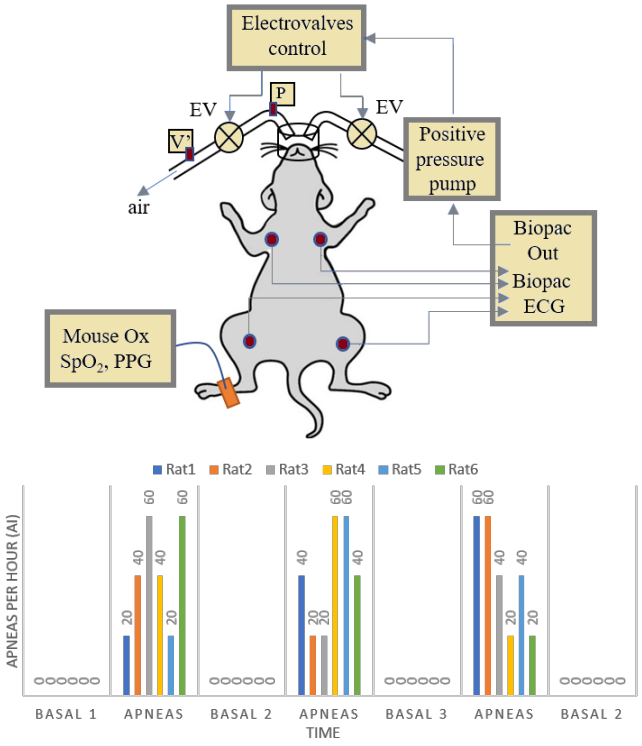

Fig. 1. a) Experiment setup for the recurrent OSA model. V': respiratory flow and (P) pressure, SpO_2 and PPG (with MouseOx Plus) and ECG (with Biopac ECG). b) Protocol: Sequences of recurrent apnea episodes applied for 15-min intervals, preceded and followed by 15-min periods of normal breathing (Basal #), applied for each rat.

During the simulated sequences of recurrent OSA episodes and spontaneous breathing, several physiological signals were acquired including respiratory flow signal, respiratory pressure and two electrocardiogram (ECG) channels (leads I and II) using Biopac® Systems. SpO_2 and photoplesthysmography signal were measured by a pulse oximeter (Mouse OxPlus®) attached in the rat leg (see Fig 1-a).

B. Experimental Protocol

In the protocol used for this experiment, recurrent apnea episodes were induced for 15-min intervals followed by 15-min resting periods. Apnea episodes were periodically simulated at rates of 20, 40 and 60 events per hour, with each episode lasting 15 s (Fig. 1-b). The order of the applied frequency in each 15-min recurrent apnea sequences was randomly selected for each animal. Oxygen saturation drops, measured from SpO_2 signal, ranged between 5–23% with respect to the preapnea values. For this study, basal and hypoxic intervals of 10 consecutive heartbeats were extracted before and during each apnea episode, respectively, to assess ECG morphological changes due to the hypoxia provoked during the experiment.

C. ECG Preprocessing

ECG signals (lead I) were preprocessed before the estimation of the studied markers, including QRS complex detection and subsequent inspection to remove abnormal beats, baseline drift attenuation, 4^{th} order bidirectional Butterworth low pass filtering at 45 Hz to remove high frequency noise and, wave boundaries delineation using a wavelet-based tecnique [12].

D. DTW analysis of the depolarization

When using DTW approach, the involved sequences are warped in a non-linearly fashion through time dimension to estimate a surrogate measure of their similarity independent of certain non-linear variations in the time dimension. In addition to a similarity measure between the two sequences, a so called *warping path* is produced. By warping according to this path, the two signal sequences may be aligned in time. Fig. 2 shows the *warping path* obtained by this non-linear approach applied on two real QRS complex waveforms.

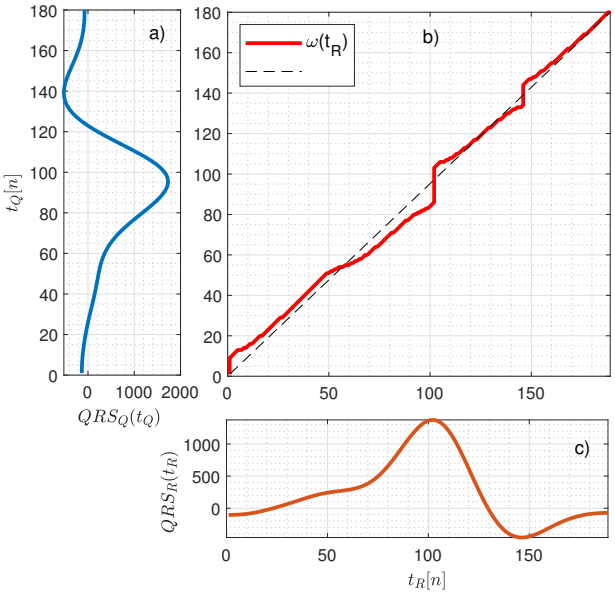

Fig. 2. Example of dynamic time warping (DTW) approach applied for two QRS waves. a) and c) represent the QRS sequences to be aligned. b) is the *warping path* $\omega(t_R)$ obtained after aligning both sequences.

In our study, the sequences to be aligned using DTW correspond to the depolarization interval (QRS complex) of two average heartbeats, as illustrated in Fig 2-(a) and (c). In brief, ten 60-ms segments corresponding to 10 consecutive heartbeats, were extracted for those periods of interest (before and during the end of the hypoxic events). These sequences, centered at QRS fiducial points, were firstly aligned via maximum cross-correlation and subsequently averaged.

Finally, the average sequences were restricted to only the onset and end points of the QRS complexes, obtaining the reference ($Q\hat{R}S_R(t_R)$) and the query ($Q\hat{R}S_Q(t_Q)$) QRS-waves. The optimal warping function, $\hat{\omega}(t_R)$, derived from aligning $Q\hat{R}S_R(t_R)$ and $Q\hat{R}S_Q(t_Q)$, is shown in Fig 2-(b).

Since the level of warping needed to optimally align two QRS waves may vary upon different situations, relevant information can be obtained regarding time-domain variability. To quantify this warping level, the mean of the absolute difference between $\omega(t_R)$ and t_R is computed [8]:

$$\Lambda_T = \frac{1}{N_r}\sum_{n=1}^{N_r} |\omega(t_R[n]) - t_R[n]| \quad (1)$$

On the other hand, the difference between $Q\hat{R}S_R(t_R)$ and $Q\hat{R}S_Q(\omega(t_R))$ due to amplitude variability can be calculated as the area bounded by $Q\hat{R}S_R(t_R)$ and $Q\hat{R}S_Q(\omega(t_R))$, normalized by the L^2-norm of $QRS_R(t_R)$:

$$\Lambda_A = \frac{e_a}{\|e_a\|}\frac{\|QRS_Q(\omega(t_R)) - QRS_R(t_R)\|}{\|QRS_R(t_R)\|} \times 100 \quad (2)$$

where the term $\frac{e_a}{\|e_a\|}$ account for the sign, being:

$$e_a = \sum_{n=1}^{N_r}(QRS_Q(\omega(t_R)) - QRS_R(t_R)) \quad (3)$$

E. Depolarization markers

To evaluate the added value of the morphological indices described above, traditional ECG markers related to ventricular depolarization, such as the amplitude of the R and S waves ($\mathcal{A}_R$, $\mathcal{A}_S$), were also assessed from the analyzed ECG signals. Furthermore, two morphological markers were extracted: the upstroke and downstroke slopes of the R wave, denoted $\mathcal{U}_R$ and $\mathcal{D}_R$, respectively. $\mathcal{U}_R$ and $\mathcal{D}_R$ are the result of fitting a straight line over the ECG signal in specific segments within the QRS complex, as described in [7].

F. Statistical analysis

Results are expressed in mean ± SD. The measures obtained before and during the hypoxic episodes were compared using the Wilcoxon signed non-parametric range test. The relationship between changes in DTW-based parameters and conventional QRS markers was determined using Pearson's correlation coefficient. The significance level was set at 0.05 in all cases.

III. RESULTS AND DISCUSSION

Figure 3 shows two representative examples of average QRS waves aligned using the DTW approach. More specifically, they illustrate the transient and overall changes in QRS morphology, caused by an isolated hypoxic episode and after completion of the entire protocol, respectively, for a particular animal. The optimal warping functions ($\hat{\omega}(t_R)$) corresponding to each example are represented in Fig 3 (c) and (d). The reference and warped QRS waves, $Q\hat{R}S_R(t_R)$ and $Q\hat{R}S_Q(\omega(t_R))$, are shown in Fig 3 (a) and (b) for both scenarios. Note that, in the case of the isolated episode (left column), the aligned waves appear to be almost identical, which is reflected in a more linear warping function. Conversely, by aligning the basal waves taken at the beginning and end of the experiment (right column), a substantial difference in morphology is observed. The warping path in this case clearly showed some contraction and expansion intervals.

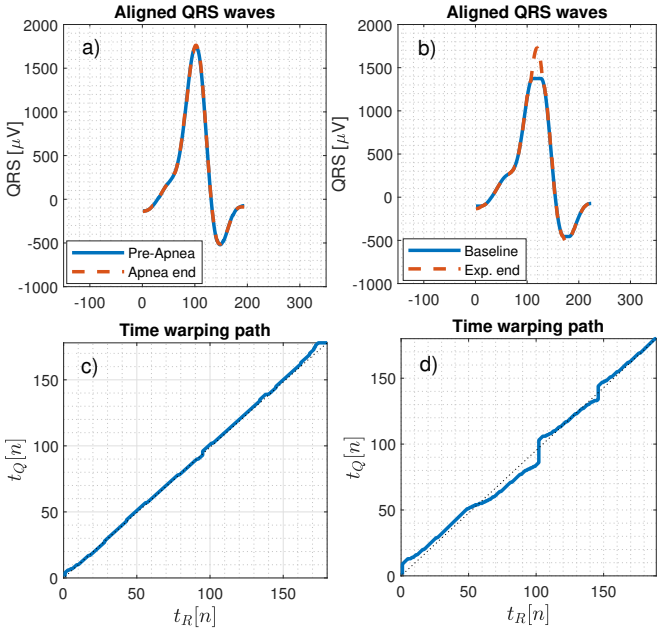

Fig. 3. Aligned QRS waves after applying the DWT technique in two different situations: a) to compare basal and hypoxic segments of an isolated episode and, b) to compare the initial and final basal segments of the experiment. c) and d): warping paths needed to align the QRS waves of (a) and (b), respectively.

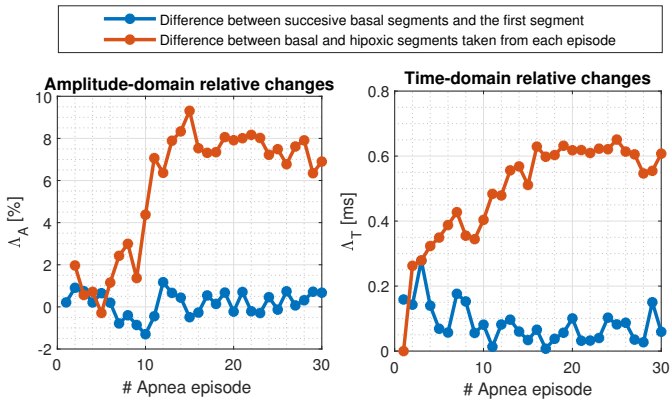

Fig. 4. Temporal evolution (in red) of Λ_A and Λ_T, from the first apnea episode to the last, during the whole duration of the protocol for a particular animal. The differences between each hypoxic segment (taken at the end of the episode) and their respective basal segments (pre-apnea segment) are also shown (in blue).

Changes computed over time in relation to the first basal value are presented in Fig 4 for Λ_A and Λ_T, where a progressive increase up to the middle of the experiment in

both amplitude (up to 8%) and duration (up to 0.6 ms) of the QRS wave is shown. Mean values for the population were 6.3±3.7 % for Λ_A and 0.74±0.15 ms for Λ_T. However, the differences between the hypoxic episodes and their respective pre-apnea segments remained around 0% (p = 0.131) in the case of Λ_A, while in the case of Λ_T are under 0.2 ms ($p < 0.001$), with higher values especially at the beginning.

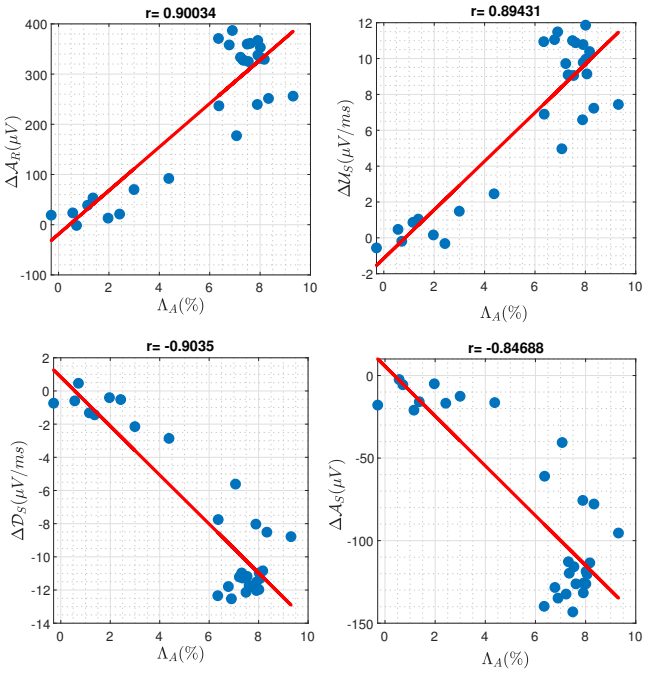

Fig. 5. Relationship between changes occurring in Λ_A and the changes in the amplitude of the R wave ($\mathcal{A}_R$), its upward and downward slopes ($\mathcal{U}_R$ $\mathcal{D}_R$) and the amplitude of the S wave ($\mathcal{A}_S$).

TABLE I

CORRELATION VALUES (MEAN ± SD) OBTAINED BETWEEN DTW-DERIVED MARKERS AND CONVENTIONAL ECG MARKERS.

Index	$\Delta\mathcal{A}_R$ (μV)	$\Delta\mathcal{A}_S$ (μV)	$\Delta\mathcal{U}_R$ (μV)	$\Delta\mathcal{D}_R$ (μV)
Λ_A (%)	0.92±0.06	-0.88 ±0.07	0.91±0.07	-0.92±0.05
Λ_T (ms)	0.74±0.33	-0.71±0.35	0.74±0.32	-0.75±0.32

Finally, it was found that the changes observed in the analyzed morphological markers were significantly correlated ($r \approx 0.9$) with the changes of the conventional QRS parameters, as shown in Fig-5 when plotting $\mathcal{A}_R$, $\mathcal{U}_R$, $\mathcal{A}_S$ and $\mathcal{D}_R$ against Λ_A. Table I summarizes the average correlation values obtained for Λ_T and Λ_T against all other QRS parameters. Interestingly, a stronger correlation was found for Λ_A compared to that obtained for Λ_T. This may suggest that Λ_A has a better capacity to track morphological variations than Λ_T, probably because hypoxia-induced amplitude changes prevail over time-domain fluctuations. Nevertheless, the latter could provide complementary information to better explain the severity of intermittent hypoxia, considering either its incidence rate or the levels of desaturation caused by the hypoxic episodes.

The results obtained in this study support the potential of the DTW method to capture global morphological changes occurring in the ECG depolarization due to recurrent hipoxia, even though these changes may be very subtle, as occurs between basal segments and hypoxic episodes. It is important to highlight that there is a crucial step in the success of such an alignment, which is mainly related to the correct delineation of the onset and end points of the temporal sequences to be aligned.

ACKNOWLEDGMENT

The authors are grateful to Ramon Farré, Daniel Navajas, Josep Maria Montserrat, Isaac Almendros, Marta Torres and Puy Ruiz for their excellent help in designing and implementing the animal model.

REFERENCES

[1] N.R. Prabhakar. Invited Review: Oxygen sensing during intermittent hypoxia: cellular and molecular mechanisms. J Appl Physiol, vol. 90, pp. 1986-1994, 2001.

[2] L. Lavie. Obstructive sleep apnoea syndrome - an oxidative stress disorder. Sleep Med Rev, vol. 7, pp. 35-51, 2003.

[3] L. Lavie. Sleep-disordered breathing and cerebrovascular disease: a mechanistic approach. Neurol Clin, vol. 23, pp. 1059–1075, 2005.

[4] E.C. Fletcher. Invited review: Physiological consequences of intermittent hypoxia: systemic blood pressure. J Appl Physiol, vol. 90, pp. 1600-1605, 2001.

[5] D. Romero, R. Jané. Non-linear HRV Analysis to Quantify the Effects of Intermittent Hypoxia Using an OSA Rat Model. In 41st Annual International Conference of the IEEE Engineering in Medicine and Biology Society (EMBC), Berlin, Germany, pp. 4994–4997, IEEE, 2019.

[6] A. Shimokawa, T. Kunitake, M. Takasaki, H. Kannan. Differential effects of anesthetics on sympathetic nerve activity and arterial baroreceptor reflex in chronically instrumented rats. J. Auton. Nerv. Syst., vol. 72, pp. 46–54, 1998.

[7] D. Romero, M. Ringborn, P. Laguna, E. Pueyo. Detection and quantification of acute myocardial ischemia by morphologic evaluation of QRS changes by an angle-based method. Journal of electrocardiology, 46(3), pp. 204–214, 2013.

[8] J. Ramírez, M. Orini, J.D. Tucker, E. Pueyo, P. Laguna. Variability of ventricular repolarization dispersion quantified by time-warping the morphology of the T-waves. IEEE Trans Biomed Eng, vol. 64, no. 7, pp. 1619–1630. 2016.

[9] R. Farré, M. Ncher, A. Serrano-Mollar, J.B. Gldiz, F.J. Alvarez, D. Navajas J.M. Montserrat. Rat model of chronic recurrent airway obstructions to study the sleep apnea syndrome. Sleep, vol. 30, pp. 930–933, 2007.

[10] A. Carreras, I. Almendros, I. Acerbi, J.M. Montserrat, D. Navajas, R. Farré. Obstructive apneas induce early release of mesenchymal stem cells into circulating blood. Sleep, vol. 32, pp. 117–119, 2009.

[11] R. Jané R, J. Lázaro, P. Ruiz, E. Gil, D. Navajas, R. Farré, P. Laguna. Obstructive Sleep Apnea in a rat model: Effects of anesthesia on autonomic evaluation from heart rate variability measures. In proc. Computing in Cardiology (CinC), pp. 1011-1014, 2013.

[12] J.P. Martínez, R. Almeida, S. Olmos, A.P. Rocha, P. Laguna. A wavelet-based ECG delineator: evaluation on standard databases. IEEE Trans Biomed Eng, vol. 51, pp. 570-581, 2004.